

## Mobility of discrete cavity solitons

O. Egorov, U. Peschel, and F. Lederer

*Institute of Condensed Matter Theory and Solid State Optics, Friedrich-Schiller-Universität Jena, Max-Wien-Platz 1, 07743 Jena, Germany*

(Received 30 June 2005; published 6 December 2005)

We investigate the mobility of discrete cavity solitons in arrays of coupled quadratic nonlinear resonators driven by an inclined holding beam. Unlike in transversely homogeneous cavities the inherent discreteness hinders or even prevents the soliton motion. As a consequence for the same system parameters one type of soliton may still be at rest, whereas others already move. This feature gives rise to collisions between these different types. To study the soliton dynamics in more detail we take advantage of a perturbation theory and derive soliton velocities semianalytically.

DOI: [10.1103/PhysRevE.72.066603](https://doi.org/10.1103/PhysRevE.72.066603)

PACS number(s): 42.65.Pc, 42.65.Tg, 42.65.Wi, 42.82.Et

### I. INTRODUCTION

Recently much emphasis has been on experimentally and theoretically studying intrinsic light localization in discrete optical systems, where an array of evanescently coupled waveguides is a typical example for such a system. The peculiarities of discrete diffraction allow for the formation of new types of spatially localized solutions, viz, so-called discrete solitons [1], which were predicted in the seminal work [2] by Christodoulides and co-workers and were later experimentally observed in media with Kerr [3], saturable cubic [4], and quadratic nonlinearities [5]. Unlike homogeneous media discrete systems lack translational invariance in the transverse direction and, as a consequence, an effective trapping potential, the so-called Peierls-Nabarro potential (PNP), appears [6]. It is a measure of the barrier, which solitons have to overcome, when moving from site to site. Actually, the PNP is the difference of the Hamiltonians of two types of localized solutions of same power, which may exist in discrete systems, namely on-site (“odd”) and intersite (“even”) discrete solitons. The PNP hinders or even completely suppresses the discrete soliton’s motion in transverse directions. Based on this effect some discrete soliton switching schemes were proposed [7].

Adding feedback and resonant enhancement to the discrete system allows for new degrees of freedom. A possible implementation is a nonlinear waveguide array with dielectric mirrors at the end faces where radiation losses are compensated for by a driving or pump field (Fig. 1). Feedback and field enhancement give rise to bi- or multistability of optical states, where the nonlinear effects require substantially less power to occur compared to a single pass configuration. Recently, the existence of localized solutions in such an array of coupled nonlinear cavities, i.e., of discrete cavity solitons (DCS), was predicted both for cubic [8] and quadratic [9] nonlinearities. Actually, for strong coupling between waveguides DCSs behave like conventional cavity solitons (CSs) known from homogeneous planar resonators where canonical (continuous) diffraction takes place (for recent reviews, see [10,11]). In particular, CS may exist on a stable and preferably flat (plane wave) background and once excited by a local change of the incident field, in principle, they stay forever, even if the initial excitation has been

switched off [12–18]. Moreover, their ability to react upon external perturbations, e.g., system parameter variations, can be used to control the position of CSs [19,20]. It was found that smooth inhomogeneities force the CS to move into the transverse direction with a velocity proportional to the local gradient of the corresponding inhomogeneity [19–21]. Unlike in the transversely homogeneous (continuous) case the dynamical properties of DCSs [8,9] have not been yet properly investigated. Due to the lack of translational invariance it might be anticipated that discreteness appreciably affects the mobility of DCS as observed in the conservative case. Recently, moving midband lattice cavity solitons have been identified but in an active medium and without the holding beam [22].

The aim of this paper is to investigate the dynamics of DCS in an array of coupled quadratically nonlinear cavities when an inclined holding beam is applied. This holding beam acts like a force triggering a transverse motion. But the lack of translational symmetry caused by the very discreteness of the system counteracts this force. Thus, in contrast to the continuous case where cavity solitons start to move for an arbitrary small inclination, DCS to move require a certain threshold inclination. Below this threshold DCS just rest at definite sites in the discrete system. Thus the interplay of these two effects, namely the holding beam inclination and the trapping caused by discreteness, will determine the dynamics of DCSs.

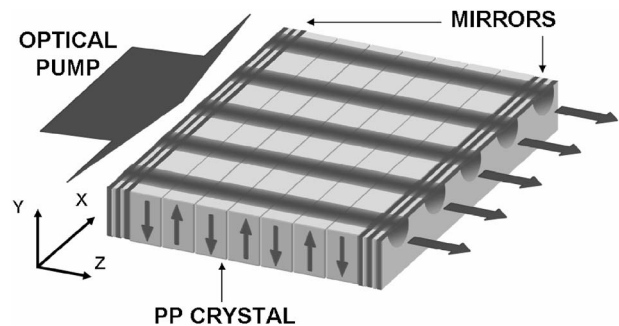


FIG. 1. Array of evanescently coupled nonlinear cavities driven by an external field. The PPLN waveguides are coated with highly reflected Bragg mirrors.

The paper is organized as follows: In Sec. II we derive the “continuous limit” of the mean-field equations valid for wide DCSs and calculate the soliton velocity as it depends on the holding beam inclination. This continuous model serves as an approximation to the very discrete one by using the standard continuous equations but some peculiarities of discrete diffraction included. Then, in Sec. III, by using this model for the calculation of zero-order solutions we describe analytically the critical gradient (threshold) of the holding beam which triggers transverse soliton motion. It turns out that the “quasitranslational” mode, which is the discrete analog of the neutral or translational mode of the continuous model, determines the dynamics of solitons in the discrete system. In a next step we show that for identical system parameters one DCS type may be at rest, whereas others already move. This feature gives rise to collisions between these different soliton types. The results of interaction of moving and resting solitons are discussed in Sec. IV.

## II. THE MODEL

An experimental study of DCS could rely on a configuration recently used for discrete soliton formation, namely a periodically poled lithium niobate (PPLN) waveguide array [5] but coated with highly reflecting Bragg mirrors at the end faces (see Fig. 1). Typical data of this sample are a length of 10 mm, a channel separation of 10–20  $\mu\text{m}$ , and a waveguide width of 7  $\mu\text{m}$ . A rough estimation yields that an input power of 5 mW per channel at a cavity finesse of about 50 is sufficient for cavity soliton formation.

We assume that the cavities are resonant for both the fundamental frequency (FF) and second harmonic (SH) waves and that a mean-field approach can be applied. The detailed derivation of the mean-field model as well as the discussion of its limits can be found elsewhere [9]. The radiation losses are compensated for by an external FF driving field. Here, we restrict ourselves to a quasi-infinite array of identical evanescently coupled high- $Q$ -cavities. The appropriately scaled evolution equations for the slowly varying envelopes of the transmitted FF and SH fields read as [9]

$$i \frac{\partial u_n}{\partial T} + C_1(u_{n-1} + u_{n+1} - 2u_n) + (i + \Delta_1)u_n + u_n^* v_n = E_0 e^{iqn},$$

$$i \frac{\partial v_n}{\partial T} + C_2(v_{n-1} + v_{n+1} - 2v_n) + (i\delta + \Delta_2)v_n + u_n^2 = 0, \quad (1)$$

where  $\Delta_{1,2}$  are detunings of both fields from the cavity resonance scaled in terms of the resonance width at the FF. The time  $T$  is scaled with the FF photon lifetime and  $\delta$  is the ratio of the FF/SH photon lifetimes,  $C_{1,2}$  are the normalized FF/SH coupling constants. Usually  $C_1 \gg C_2$  holds because in realistic experimental situations SH field profiles are much stronger confined compared to FF ones and the corresponding overlap integrals are much less (see for example [5]). We also allow for an inclination of the holding beam (amplitude  $E_0$ ) by introducing a phase shift  $q$  between the field incident on adjacent cavities.

For normal incidence ( $q=0$ ) the system (1) possesses stationary localized solutions. Details regarding the properties

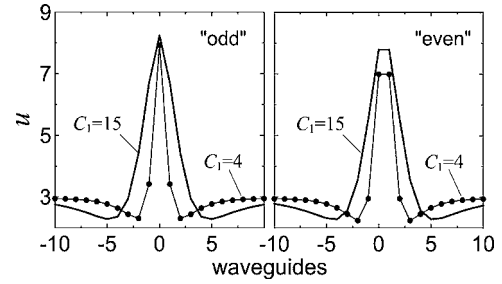


FIG. 2. The FF amplitude profiles (normalized units) of odd and even bright DCSs for different coupling constants.  $E_0=11.2$ ,  $\Delta_1=-5$ ,  $\Delta_2=-6$ ,  $\delta=1$ .

of these quadratic DCSs can be found in [9], here we only concisely review the most important features. Like in the conservative case we may distinguish between two independent DCSs, namely odd and even ones (Fig. 2). The scaled coupling constant  $C_1$  can vary in a wide range where stronger coupling entails wider DCSs (see Fig. 2). For very large coupling ( $C_1 \rightarrow \infty$ , continuous limit), odd and even DCSs are identical and cover a large number of cavities.

The primary aim of this paper is to get insight into the physics of the mobility of DCSs. This can be hardly analytically achieved in dealing with the discrete set of Eq. (1). That is why we will take advantage of a continuous model which is valid for a large coupling constant ( $C_1 \rightarrow \infty$ ) but keeps several features of the discrete system. Resulting in translational symmetry it does not describe completely the peculiarities of discreteness but it will serve as a starting point for an analysis of the discrete model (1). In this case the optical field varies slowly across the array and we can introduce the continuous transverse coordinate  $x$  and functions  $u(x)$ ,  $v(x)$ , which are by definition envelopes of the discrete solution of Eq. (1):  $u(x=nh) \equiv u_n$ ,  $v(x=nh) \equiv v_n$ , where the separation between adjacent cavities  $h \equiv 1/\sqrt{C_1}$  is assumed to be a small parameter. Thus the following expansion is valid for  $C_1 \rightarrow \infty$ :  $u_{n\pm 1} \approx u_n \pm h \partial_x u + \frac{1}{2} h^2 \partial_{xx} u$ . In this continuous limit one can replace the set of coupled ordinary differential equations (1) by two partial differential equations as

$$i \frac{\partial u}{\partial T} + \frac{\partial^2 u}{\partial x^2} + (i + \Delta_1)u + u^* v = E_0 e^{ikx},$$

$$i \frac{\partial v}{\partial T} + \alpha \frac{\partial^2 v}{\partial x^2} + (i\delta + \Delta_2)v + u^2 = 0, \quad (2)$$

where  $\alpha=C_2/C_1$  and  $k=q/h$  is the phase gradient. The system (2) is identical to that which describes the evolution of the transmitted field of a Fabry-Perot cavity filled with a homogeneous quadratically nonlinear medium. But in contrast to that case, where  $\alpha \approx 0.5$  [10,12,13], here this crucial parameter  $\alpha$  can considerably vary, even for strongly coupled cavities. Thus, only  $C_1, C_2 \rightarrow \infty$  results in  $\alpha \approx 0.5$ . Physically, it can be anticipated that Eq. (2) provides moving soliton solutions for any small inclinations of the holding beam but the varying parameter  $\alpha$  reflects still that discrete diffraction is different for the FF and SH component. Considering this

effect from a more general point of view one finds that any spatial variation of a system parameter such as e.g. of the holding beam or the cavity detuning causes a motion of DCS in continuous limit (like conventional CS in [20]). This motion arises from a nonzero projection of the parameter variation onto the neutral or translational mode of the unperturbed system [19,20]. This neutral mode provokes translation. Thus, an excitation of this mode evokes a change in the position of the soliton. Actually, the velocity of the transverse motion is proportional to the gradient of the perturbation parameter. So, starting from continuous model (2) for DCSs and considering an inclination of the holding beam as the relevant parameter, we proceed with solutions of the discrete model (1) later.

### III. DYNAMICS OF DISCRETE CAVITY SOLITONS

We use perturbation theory by investigating the influence of a small inclination of the holding beam to the DCSs [19,20]. To this end we introduce real-valued quantities and rewrite Eq. (1) in the following general form:

$$\partial_T \mathbf{u} - \mathbf{w}|_{\mathbf{u}} = \mathbf{p} \quad (3)$$

with  $\mathbf{u} = (\dots, \text{Re } u_n, \text{Im } u_n, \text{Re } v_n, \text{Im } v_n, \dots)$ .  $\mathbf{w}$  is a nonlinear vector functional and  $\mathbf{p} = (\dots, E_0 q n, 0, 0, 0, \dots)$  is a small perturbation, induced by the phase shift  $q$  of the holding beam in first-order approximation. Assuming that the perturbation is of order  $\varepsilon \ll 1$  and the field scales as  $\mathbf{u} = \mathbf{u}_0 + \varepsilon \mathbf{u}_1 + \dots$ , we get from Eq. (3) in first order in  $\varepsilon$ ,

$$\partial_T \mathbf{u}_1 - \partial_{\mathbf{u}} \mathbf{w}|_{\mathbf{u}_0} \mathbf{u}_1 = \mathbf{p}, \quad (4)$$

where  $\partial_{\mathbf{u}} \mathbf{w}|_{\mathbf{u}_0}$  is the Jacobian of Eq. (3) obtained by linearizing around the stationary solution  $\mathbf{u}_0$ . Expanding the perturbation with respect to the basis of eigenvectors of this Jacobian  $\mathbf{u}_1 = \sum_i a_i(T) \boldsymbol{\psi}_i$  we get the following set of evolution equations for the amplitudes of each eigenvector:

$$\partial_T a_i(T) - \lambda^i a_i(T) = \frac{\boldsymbol{\psi}_i^+ \cdot \mathbf{p}}{\boldsymbol{\psi}_i^+ \cdot \boldsymbol{\psi}_i}, \quad (5)$$

where  $\boldsymbol{\psi}_i^+$  is the eigenvectors of the adjointed Jacobian  $\partial_{\mathbf{u}} \mathbf{w}^+|_{\mathbf{u}_0}$ .

As it was shown above the continuous model (2) is mathematically equivalent to the discrete one (1) provided that the FF coupling constant converges to infinity ( $C_1 \rightarrow \infty$ ). Due to the translational symmetry of the continuous model (2) one of the eigenvectors of  $\partial_{\mathbf{u}} \mathbf{w}|_{\mathbf{u}_0}$  is proportional to the spatial derivative of the stationary solution  $\boldsymbol{\psi}_{\text{tr}} = \partial_x \mathbf{u}_0$  and possesses a zero eigenvalue ( $\lambda^{\text{tr}} = 0$ ). This is so-called neutral or translational mode. An excitation of this eigenvector  $\mathbf{u} = \mathbf{u}_0 + a \partial_x \mathbf{u}_0$  results in a spatial displacement because any solution  $\mathbf{u}_0$ , which is shifted by  $\Delta x$  can be expressed by a Taylor expansion,  $\mathbf{u}(x + \Delta x) \approx \mathbf{u}_0 + \Delta x \partial_x \mathbf{u}_0$ . Therefore the amplitude of the translational mode  $a_{\text{tr}}$  can be regarded as a spatial shift  $\Delta x$  and in accordance with Eq. (5) the instantaneous DCSs velocity in the continuous limit is

$$V_0 = \partial_T \Delta x = \frac{\boldsymbol{\psi}_{\text{tr}}^+ \cdot \mathbf{p}}{\boldsymbol{\psi}_{\text{tr}}^+ \cdot \boldsymbol{\psi}_{\text{tr}}}. \quad (6)$$

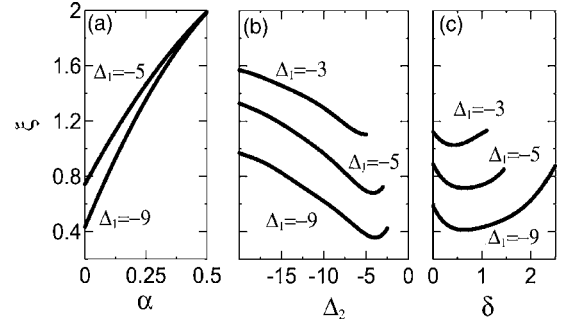


FIG. 3. The mobility coefficient  $\xi$  of a bright DCS in the continuous limit ( $V_0 = \xi k$ , where  $V_0$  is the soliton velocity for a phase gradient  $k$  of the holding beam). Parameters: (a)  $\Delta_2 = -6$ ,  $\delta = 1$ ; (b)  $\alpha = 0$ ,  $\delta = 1$ ; (c)  $\Delta_2 = -6$ ,  $\alpha = 0$ .

The DCS carries other modes as well, which might be excited simultaneously. Usually in dissipative systems [13,19] all eigenvectors but the translational one have eigenvalues with negative real part, thus they are damped exponentially indicating stable stationary solutions. Moreover, only the translational mode  $\boldsymbol{\psi}_{\text{tr}}$  contributes to a spatial displacement. Therefore we solely concentrate on its excitation.

The expression for the DCS velocity (6) was obtained for the well studied case of canonical paraxial diffraction [10,20]. Unlike in this case discrete diffraction laws can change the mobility properties of DCS even in the continuous limit (2). Here, as a matter of fact, the ratio of diffraction coefficients of SH and FF fields ( $\alpha$ ) may considerably deviate from  $\alpha = 0.5$ . For the canonical paraxial diffraction ( $\alpha = 0.5$ ) the inclination of the holding beam can be transformed away by introducing a constant velocity  $V_0 = 2k$ . The very reason for this is that both the FF and SH beams exhibit the same refraction properties, i.e., transverse velocities of the spatial envelopes. But for the general case ( $\alpha \neq 0.5$ ), the transverse velocity of the DCS consisting of a FF and SH component will attain values in an interval set by the two velocities of FF and SH field, respectively. It will turn out that DCS mobility strongly depends on the ratio of the amplitudes of both harmonics and, therefore, the system parameters. Assuming a linear relation  $V_0 = \xi k$  between a phase gradient and the velocity the ‘‘mobility’’ coefficient  $\xi$  can be calculated by means of direct numerical integration of Eq. (2). (Fig. 3). Indeed, being  $\xi = 2$  for the paraxial case ( $\alpha = 0.5$ ) the mobility coefficient decreases for vanishing SH diffraction [Fig. 3(a)]. From Fig. 3(b) it is evident that the bright DCS becomes more mobile for small FF ( $\Delta_1$ ) and large SH detunings ( $\Delta_2$ ), respectively. In this case the SH field is weak and, therefore, the quadratic nonlinearity can be mimicked by a complex valued cubic one. Provided that the FF field plays the major role the mobility coefficient converges to  $\xi = 2$  (like for cavity solitons in a cubic nonlinearity [21]). The ratio of photon lifetimes  $\delta$  affects the mobility of DCS as well [Fig. 3(c)]. The decrease of SH amplitude can again explain the increase of the mobility coefficient  $\xi$  for large SH losses ( $\delta$ ).

Now we proceed with the full discrete model (1) starting with a large FF coupling constant  $C_1$ , which should almost reproduce the result obtained from the continuous model (2).

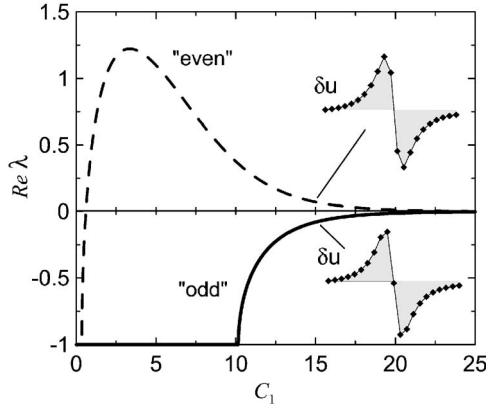


FIG. 4. The growth rate of the quasitranslational mode vs the coupling constant for odd (solid line) and even (dashed line) bright DCSs.  $E=11.2$ ,  $\Delta_1=-5$ ,  $\Delta_2=-6$ ,  $\delta=1$ .

As in a realistic array we set  $C_2 \rightarrow 0$ . If a DCS starts moving, it has to jump from site to site while transforming its shape periodically. To a certain extent this transformation can be envisaged as a permanent transition between odd and even solutions. Therefore, one can anticipate that DCS mobility is directly affected by the stability properties of the respective resting solutions, which it has to pass. Seeking for solutions in the form  $\mathbf{u} = \mathbf{u}_0 + \delta \mathbf{u} e^{\lambda T}$  and linearizing Eq. (1) around the stationary solution  $\mathbf{u}_0$  with respect to a small perturbation  $\delta \mathbf{u}$  we calculate the eigenvalue spectra for both odd and even DCSs. The eigenvalue with the largest real part converges to zero for increasing coupling constant (Fig. 4). In this case the corresponding quasitranslational mode coincides with the neutral or translational mode in the continuous limit ( $C_1 \rightarrow \infty$ ). Thus only this mode is important for the soliton stability provided that the coupling constant is large enough. For example a bright even solution destabilizes ( $\lambda^{\text{even}} > 0$ ) due to the growth of the quasitranslational mode (see [9]). By contrast the odd DCS remains stable ( $\lambda^{\text{odd}} < 0$ ).

The system (1) lacks translational symmetry and, therefore, the eigenvalue of the quasitranslational mode is non-zero. On the other side we still assume, like in the continuous limit, that the amplitude of the quasitranslational mode determines the spatial displacement from a stationary solution. As a result using Eq. (5) we get the approximate expression for the local velocity in the vicinity of odd (even) DCS,

$$V = \partial_T \Delta x = \lambda^{\text{odd(even)}} \Delta x + V_0, \quad (7)$$

where  $\lambda^{\text{odd(even)}}$  is the eigenvalue of the quasi-translational mode and  $\Delta x = x - x_{\text{odd(even)}}$  is the shift from the DCS center.  $V_0$  is the velocity [Eq. (6)] known in first order from the continuous model. Odd DCSs are centered at a cavity and thus this center is located at  $x_{\text{odd}}/h = 0, 1, \dots$ , whereas the even DCS is situated between sites  $x_{\text{even}}/h = 0.5, 1.5, \dots$ . Equation (7) describes a velocity of DCS in the vicinity of odd and even soliton positions  $x_{\text{odd}}, x_{\text{even}}$  (dashed lines in Fig. 5). Then we are looking for a continuous function which connects smoothly all this points. We use a linear combination of two sine-functions, which satisfies Eq. (7) by means of its Taylor expansion around soliton centers. So the instan-

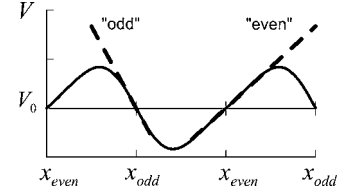


FIG. 5. The instantaneous velocity  $V$  of a DCS in discrete model (1) depending on the soliton position  $x$ . Dashed lines describe the results of the perturbation analysis around odd (even) DCSs [Eq. (7)]. The solid line corresponds to the continuous approximation (8).  $V_0$  is the velocity calculated in the continuous model (2).

taneous velocity for any continuous  $x$  is approximated as (solid line in Fig. 5),

$$V = \lambda^- \sin(2\pi x/h) + \lambda^+ \sin(4\pi x/h) + V_0(q), \quad (8)$$

where  $\lambda^- = (\lambda^{\text{odd}} - \lambda^{\text{even}})h/4\pi$ ,  $\lambda^+ = (\lambda^{\text{odd}} + \lambda^{\text{even}})h/8\pi$ ;  $\lambda^{\text{odd}}, \lambda^{\text{even}}$  are the real eigenvalues of the quasitranslational mode of odd and even DCSs, respectively and  $V_0(q)$  is the DCS velocity in the continuous model (2). Keeping in mind that  $V_0(q) = \xi k = \xi q/h$  the parameter  $V_0(q)$  can be easily related to the phase shift  $q$ . The coefficients  $\lambda^\pm$  in Eq. (8) are mathematical guesses, which allow us to satisfy Eq. (7). The first sin-term ( $\lambda^-$ ) reflects the fact that stable odd and unstable even solutions alter periodically along  $x$ . It describes effectively the growth-rate range of the quasitranslational mode, which is responsible for the soliton motion. Therefore, this term determines the critical gradient of the holding beam, which implies the transverse motion of the DCS. Equation (8) represents now the velocity, which is exerted on the DCS by the waveguide array and the phase gradient.

According to Eq. (8) moving DCSs drift into the direction of the gradient, while performing additional oscillations when jumping from waveguide to waveguide (see inset of Fig. 6). Therefore it is convenient to describe the soliton motion by an average velocity  $W = h/\Delta T$ , where  $h$  is the lattice period which is passed by the soliton during a time  $\Delta T$ . The second term in Eq. (6) can be neglected compared to the first one ( $\lambda^- \gg \lambda^+$ ) because the eigenvalues  $\lambda^{\text{odd}}, \lambda^{\text{even}}$  usually have opposite signs (Fig. 4). Then we get from Eq. (8) a simple expression for the average velocity,

$$W \cong \sqrt{V_0(q)^2 - (\lambda^-)^2} \text{ for } V_0(q)^2 \geq (\lambda^-)^2 \text{ and } W = 0 \text{ else.} \quad (9)$$

For sufficiently large coupling there is a good agreement of the velocities obtained by a direct numerical solution of Eq. (1) and from Eq. (9) (see, for example,  $C_1 = 15$  in Fig. 6). The values  $W/h$  and  $V_0/h$  in Fig. 6 represent the average number of sites which moving DCS pass during FF photon lifetime in the discrete and continuous models, respectively. It follows from Eq. (9) that DCS rest unless the inclination of holding beam exceeds some critical value which corresponds to a phase shift,

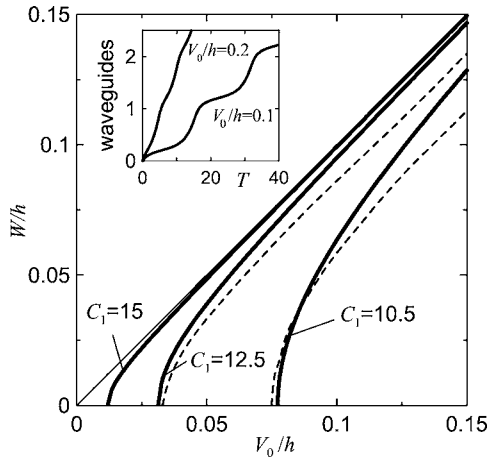


FIG. 6. The average velocity of bright DCS  $W$  vs the scaled phase gradient  $V_0 = \xi k$  for different coupling constants.  $W/h$  and  $V_0/h$  represent the average number of sites which moving DCS pass during FF photon lifetime in the discrete and continuous models, respectively. The solid lines show the results of the analytical approach (9), whereas the dashed lines are the outcome of direct numerical simulations of Eq. (1).  $E=11.2$ ,  $\Delta_1=-5$ ,  $\Delta_2=-6$ ,  $\delta=1$ . Inset: evolution of the DCS centre for different phase gradients and  $C_1=10.5$ .

$$q_{cr} = \frac{|\lambda^{odd} - \lambda^{even}|}{4\pi\xi C_1}. \quad (10)$$

Evidently, the critical shift is proportional to the eigenvalue difference of the respective odd and even soliton solutions. It decreases with increasing coupling constant and becomes zero in the continuous limit. Note that the other system parameters, like e.g. detunings, determine the mobility coefficient  $\xi$  calculated above in model (2) (see Fig. 3). Equation (10) describes almost exactly the critical gradient (critical phase shift between nearest cavities) of the holding beam provided that the respective eigenvalues are real (see  $C_1 > 10$  in Figs. 4 and 7). But the analytical approximations [Eqs. (8) and (9)] cease to hold, if the influence of discreteness grows too large. This happens if either the coupling gets

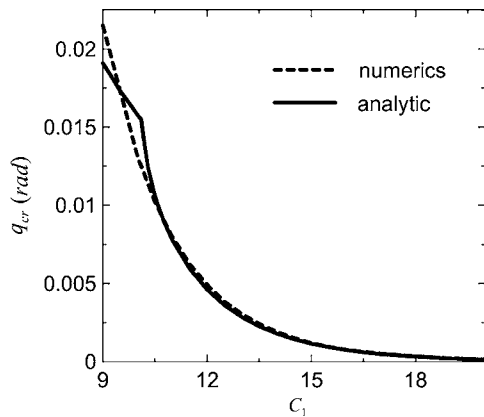


FIG. 7. Critical phase shift ( $q_{cr}$ ) between adjacent sites of the holding beam for a bright DCS [solid line: analytical approach (10)].  $E=11.2$ ,  $\Delta_1=-5$ ,  $\Delta_2=-6$ ,  $\delta=1$ .

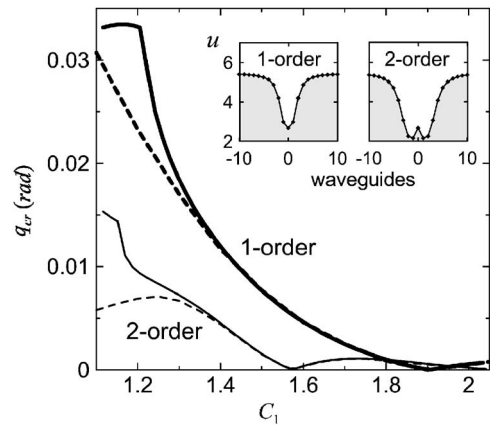


FIG. 8. Critical phase shift ( $q_{cr}$ ) between adjacent sites of the holding beam for fundamental and second-order dark DCSs. Solid lines correspond to the analytical approach (10), whereas the dashed lines are the outcome of direct numerical simulations of Eq. (1). Inset: FF amplitude profiles of the fundamental and second-order dark DCSs for  $C_1=2$ ,  $E=9.8$ ,  $\Delta_1=5$ ,  $\Delta_2=6$ ,  $\delta=1$ .

too small (continuous model ceases to be a sufficiently good zero-order solution) or the inclination of the beam grows such that the large induced phase difference  $q$  between adjacent sites requires genuine discrete diffraction to be taken into account.

This, on the other hand, provides the opportunity to use the inclination of the holding beam as a switching parameter. Solitons will move if the gradient exceeds the critical value, which depends on the coupling strength (see Fig. 7), or stay at rest otherwise. This dynamical behavior seems to be rather general for all localized solutions. We performed a similar analysis for dark DCSs by calculating the respective critical phase shift between adjacent sites  $q_{cr}$  of the holding beam (Fig. 8). In the case of multistability we find fundamental and second-order dark DCSs to coexist for the same set of system parameters (see profiles in the inset of Fig. 8). However, respective critical angles of inclination, which force the structures to move, are different (see Fig. 8). For a particular set of parameters (see  $C_1 \approx 1.9$  for fundamental and  $C_1 \approx 1.58$  for 2-order solitons in Fig. 8) we also found the critical gradient  $q_{cr}$  of motion to reach zero. It is intriguing that in spite of quite small coupling (discreteness matters) the mobility of dark DCSs compares to that in the translational symmetric continuous case. Approximation (10) confirms this fact (solid lines in Fig. 8) and illuminates the deeper

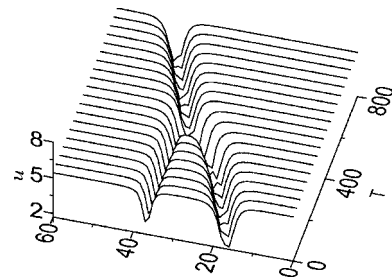


FIG. 9. Collisions between resting and moving dark DCSs with parameters:  $q=0.025$ ,  $C=1.1$ ,  $E=9.8$ ,  $\Delta_1=5$ ,  $\Delta_2=6$ ,  $\delta=1$ .

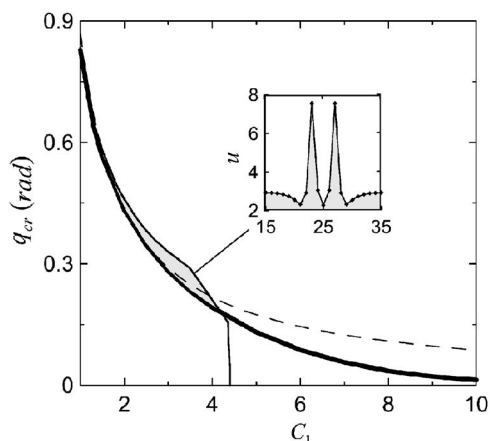


FIG. 10. Critical phase shift ( $q_{cr}$ ) between adjacent sites of the holding beam for bright DCSs (thick solid line) and two-soliton bound state (thin solid line). The thin dashed line is the empirical approximation  $q=s/C_1$ . Inset: profile of the stable two-soliton bound state,  $E=11.2$ ,  $\Delta_1=-5$ ,  $\Delta_2=-6$ ,  $\delta=1$ .

reason for this peculiar behavior. For these particular parameter values the eigenvalues of the quasitranslational modes of odd and even DCSs cross simultaneously zero ( $\lambda^{\text{odd}}=0$ ,  $\lambda^{\text{even}}=0$ ). Hence, the effective barrier vanishes and DCSs become as mobile as their continuous counterparts.

#### IV. INTERACTION OF DISCRETE CAVITY SOLITONS

As we have pointed out the mobility of DCSs is very sensitive to the tilt of the holding beam, in particular, close to the critical angle. In case of multistability coexisting structures usually have different critical angles and move with different velocities. In what follows we always assume that various types of coexisting DCSs have already been excited by initially applying appropriately shaped beams at respective positions. We now concentrate on the mobility and the interaction of these DCSs. For example the second-order dark DCS is more mobile than the fundamental one (see Fig. 8). It means that there is an interval of phase gradients, for which moving and resting DCSs exist simultaneously. This opens up the way for provoking various scenarios of soliton collisions. First we examined the interaction between moving second-order and resting fundamental dark solitons provided that an appropriate inclination of the holding beam has been applied. In this case the moving dark DCS erases the stationary one in the course of interaction (Fig. 9). It takes several hundred photon lifetimes to realize such soliton switching for an initial soliton separation of about 20 cavity spacings. This is a typical example for an inelastic interaction characteristic for dissipative systems.

However, others scenarios of soliton switching can be observed too. To prove this we have studied collision of bright localized structures for rather small coupling. Although the analytical result (10) is not valid in this domain (Fig. 10) we empirically found the critical phase gradient to be proportional to the inverse FF coupling ( $q=s/C_1$ , where  $s$  is a constant). Bright DCSs can form a stable two-soliton bound

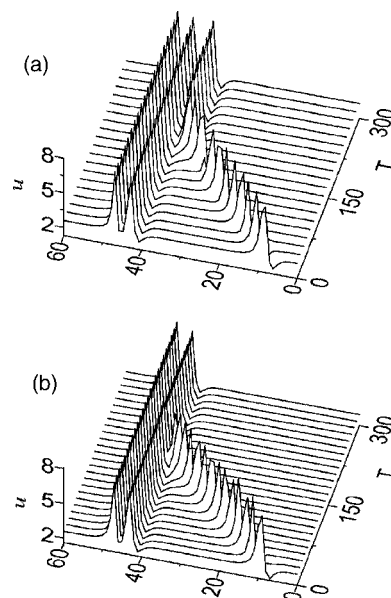


FIG. 11. Collisions between resting and moving bright DCSs; (a)  $q=0.26$  and (b)  $q=0.28$ ; other parameters:  $C=3.5$ ,  $E=11.2$ ,  $\Delta_1=-5$ ,  $\Delta_2=-6$ ,  $\delta=1$ .

state in that extremely discrete case of small coupling (see profile in the inset of Fig. 10). Note that the bound state of CSs does not exist in the continuous model (2) for this set of system parameters. Therefore it transforms into the fundamental one if the coupling constant exceeds some maximal value ( $C_1 \approx 4.2$ ). The numerical simulations of Eq. (1) show that the double-hump localized solution breaks up to a pair of moving DCSs provided that the inclination of the holding beam is large enough. The corresponding critical value of the phase gradient exceeds the critical gradient of the single DCS up to its sudden drop close to the limiting point of the double-hump soliton existence ( $C_1 < 4.2$ , Fig. 10). Therefore for some inclination the double-hump DCS rests while the single-hump DCS already moves (shaded area in inset of Fig. 10). According to our simulations there are two scenarios of bright DCS switching depending on the phase gradient. In the first one the resting structure integrates the moving soliton resulting in the formation of the multihump pattern with an additional peak [Fig. 11(a)]. Another case can be observed for a slightly larger phase gradient near the critical value for the double-hump structure. The resting soliton now absorbs the moving one during interaction [Fig. 11(b)].

#### V. CONCLUSION

In conclusion, we have analyzed the mobility properties of different types of solitons in an array of coupled cavities under the influence of an inclined holding beam, both numerically and analytically. Close to the continuous limit the critical phase gradient that forces solitons to move is almost exactly described by a simple analytical expression (10). In the case of multistability coexisting DCSs move with different velocities. Resting and moving structures allow for various types of interactions.

- [1] F. Lederer, S. Darmanyan, and A. Kobaykov, "Discrete solitons," in *Spatial Solitons*, edited by S. Trillo and W. Torruellas (Springer, New York, 2001).
- [2] D. N. Christodoulides and R. I. Joseph, "Opt. Lett. **13**, 794 (1988).
- [3] H. S. Eisenberg, Y. Silberberg, R. Morandotti, A. R. Boyd, and J. S. Aitchison, "Phys. Rev. Lett. **81**, 3383 (1998).
- [4] J. W. Fleischer, T. Carmon, M. Segev, N. K. Efremidis, and D. N. Christodoulides, Phys. Rev. Lett. **90**, 023902 (2003).
- [5] R. Iwanow, R. Schiek, G. I. Stegeman, T. Pertsch, F. Lederer, Y. Min, and W. Sohler, Phys. Rev. Lett. **93**, 113902 (2004).
- [6] Y. S. Kivshar and D. K. Campbell, Phys. Rev. E **48**, 3077 (1993).
- [7] R. A. Vicencio, M. I. Molina, and Y. S. Kivshar, Opt. Lett. **28**, 1942 (2003).
- [8] U. Peschel, O. Egorov, and F. Lederer, Opt. Lett. **29**, 1909 (2004).
- [9] O. Egorov, U. Peschel, and F. Lederer, Phys. Rev. E **71**, 056612 (2005).
- [10] D. Michaelis, U. Peschel, C. Etrich, and F. Lederer, IEEE J. Quantum Electron. **39**, 255 (2003).
- [11] U. Peschel, D. Michaelis, and C. O. Weiss, IEEE J. Quantum Electron. **39**, 51 (2003).
- [12] C. Etrich, U. Peschel, and F. Lederer, Phys. Rev. Lett. **79**, 2454 (1997).
- [13] D. V. Skryabin, Phys. Rev. E **60**, R3508 (1999).
- [14] W. J. Firth, A. J. Scroggie, Phys. Rev. Lett. **76**, 1623 (1996).
- [15] S. Barland, J. R. Tredicce, M. Brambilla, L. A. Lugiato, S. Balle, M. Giudici, T. Maggipinto, L. Spinelli, G. Tissoni, T. Knoedl, M. Miller, and R. Jaeger, Nature **419**, 699 (2002).
- [16] G. Tissoni, L. Spinelli, M. Brambilla, T. Maggipinto, I. M. Perrini, and L. A. Lugiato, J. Opt. Soc. Am. B **16**, 2095 (1999).
- [17] V. B. Taranenko, G. Sleky, and C. O. Weiss, Chaos **13**, 777 (2003).
- [18] M. Brambilla, L. A. Lugiato, F. Prati, L. Spinelli, and W. J. Firth, Phys. Rev. Lett. **79**, 2042 (1997).
- [19] T. Maggipinto, M. Brambilla, G. K. Harkness, and W. J. Firth, Phys. Rev. E **62**, 8726 (2000).
- [20] S. Fedorov, D. Michaelis, U. Peschel, C. Etrich, D. V. Skryabin, N. Rosanov, and F. Lederer, Phys. Rev. E **64**, 036610 (2001).
- [21] M. Haelterman and G. Vitrant, J. Opt. Soc. Am. B **9**, 1563 (1992).
- [22] K. Staliunas, Phys. Rev. Lett. **91**, 053901 (2003).